Optical Materials 31 (2008) 445–450

Contents lists available at ScienceDirect

Optical Materials

journal homepage: www.elsevier.com/locate/optmat

Investigation on structure and optical properties of Er^{3+}, Eu^{3+} single-doped Na_2O–ZnO–B_2O_3–TeO_2 glasses

Yanmin Yang [a,b], Baojiu Chen [a,b,*], Cheng Wang [b], Haiyang Zhong [a], Lihong Cheng [a], Jiashi Sun [a], Yong Peng [a], Xiangqing Zhang [a]

[a] Department of Physics, Dalian Maritime University, Dalian 116026, China
[b] Laboratory of Excited State Processes, Changchun Institute of Optics, Fine Mechanics and Physics, Chinese Academy of Sciences, Changchun 130033, China

ARTICLE INFO

Article history:
Received 2 November 2007
Received in revised form 18 June 2008
Accepted 19 June 2008
Available online 8 August 2008

Keywords:
Molar volume
Glass structure
Non-radiative relaxation
Up-conversion
Down-conversion

ABSTRACT

Er^{3+}, Eu^{3+} single-doped several glasses with various composition xB_2O_3–$(80-x)TeO_2$–10ZnO–$10Na_2O$ (x increases by a step of 10) were prepared by a melt-quenching technique. The effects of composition on density, molar volume, refractive index, and phonon sideband spectra were investigated. The dependence of glass structure properties on the composition was discussed. The influence of composition on the radiative and non-radiative relaxation rate, lifetime, and quantum efficiency of the level $^4I_{13/2}$ of Er^{3+} in these various glasses were studied. Upon 980 nm excitation, the composition dependence of up-conversion and down-conversion emission was studied.

1. Introduction

Er^{3+} doped telluride glass is one of the best candidates for optical communication materials owing to their high refractive index, large resistance against corrosion, high solubility of rare-earths (RE) and good transparency in the region from visible to infrared (0.35–6 μm) [1,2]. However, the excited state absorptions from $^4I_{11/2}$ level to the upper levels are very strong due to the relatively low phonon energy (around 750 cm^{-1}), thus leading to a lower infrared emission yield. Some effective approaches were proposed to overcome this drawback, for instance, introducing some helpful dopants such as Ce^{3+} to depopulate $^4I_{11/2}$ level [3]; adopting some host adjuster such as GeO_2, B_2O_3 [4–6] to increase the non-radiative transition rate of $^4I_{11/2}$ level. B_2O_3 is a good host component due to its features that does not reduce the spectral bandwidth of $^4I_{13/2}\rightarrow{}^4I_{11/2}$ transition and does not deteriorate the optical, thermal or chemical durability of the glass system. Despite the great interest in the borate–tellurite glasses as the best candidate for optical communication materials, the detailed structural information regarding the Na_2O–ZnO–B_2O_3–TeO_2 system has not been reported yet. As known that glass host composition and structure affect remarkably the optical properties, it is possible for making chemical tailoring of glass according to technological need. Thus, it is essential to study systematically the structure–composition relationship and the influence of compositions on the optical properties.

In the past decades, a lot of efforts have been made to investigate the structure of the binary sodium silicate (SS), sodium borate (SB) and ternary sodium borosilicate (SBS) [7–23]. It is well known that the structural units of the SS glasses are SiO_4 tetrahedron linking with each other by bridging oxygen, and the non-bridging oxygen (NBO) increases proportionally to the sodium ions concentration. The SB glasses consist of B–O network, built up from planar three-coordinated boron atoms and four-coordinated boron atoms. Pure B_2O_3 contains only three-coordinated boron atoms, and some of these units are transformed into four-coordinated tetrahedral as the alkali oxide content increases. The amorphous network is built by BO_3 and BO_4 groups linked by bridging oxygen atoms. The fraction of boron atoms that is four-coordinated, N_4, increases with increasing alkali oxide concentration in the region over 33%, and the non-bridging oxygen (NBO) atoms are formed, N_4 decreases [7–19]. In the SBS glasses the structure–composition relationship is more complicated than that of the SS and SB glasses, and a lot of models were raised to explain the relationship in the past several years [20–23]. A very popular model is the one established by Dell et al. [23]. In this model the ternary system is described as the binary alkali borate system diluted in the pure silica in the compositional range $R < 0.5$ and $K < 8$ (here R is the molar ratio of Na_2O/B_2O_3 and K is the molar ratio of SiO_2/B_2O_3). For $R > 0.5$, a mixing of the silica and borate portions of the glasses

* Corresponding author. Address: Department of Physics, Dalian Maritime University, Dalian 116026, China. Tel./fax: +86 411 84728909.
E-mail address: chenmbj@sohu.com (B. Chen).

0925-3467/$ - see front matter Crown Copyright © 2008 Published by Elsevier B.V. All rights reserved.
doi:10.1016/j.optmat.2008.06.014

starts with the formation of reedmergnerite group ($NaBSi_4O_{10}$). More detailed discussions have been done by Lianmeng Zhang et al. [14]. In addition, several binary tellurate glasses are reported too [24–28]. It is widely accepted that introducing small content of some modifiers into the TeO_2 glass increases the fraction of the TeO_3 groups as well as results in the formation of TeO_{3+1} polyhedron having one non-bridging oxygen atom in the TeO_2 glass.

In our previous work [29], the optical transition properties of Er^{3+} doped xB_2O_3–$(80-x)TeO_2$–10ZnO–$10Na_2O$ glasses were studied in the framework of Judd–Ofelt theory. In this present study, we investigate the glass structure, phonon sideband energy of Eu^{3+} doped these glasses, the non-radiative relaxation, the up-conversion and down-conversion luminescence of Er^{3+} doped these glasses.

2. Experimental

2.1. Sample preparation

Glasses with composition xB_2O_3–$(80-x)TeO_2$–10ZnO–$10Na_2O$ and extra $0.5Er_2O_3$ or $1Eu_2O_3$ (here $x = 10, 20, 30, 40, 50, 60, 70, 80$) were prepared by using analytical grade B_2O_3, TeO_2, ZnO, Na_2CO_3, Er_2O_3 and Eu_2O_3 as starting materials. According to a certain stoichiometric ratio the starting materials were weighted and mixed together. Each batch was well ground and put in an alumina crucible and then melted at 1150 °C for 0.5 h in a muffle furnace. Subsequently, the melts were poured into the pre-heated brass molds and annealed at 300 °C for 15 h. The glass samples were cut and carefully polished to meet the optical measurement. Each sample looks better transparent. According to the different composition, the samples were numbered as T[(80−x)/10]B(x/10), where x represents the same meaning as mentioned above. A detailed preparation procedure could be found in our previous work [29].

2.2. Characterization

The refractive indexes for all the samples were measured by using an UVISEL SPME ellipsecopy. Glass densities were obtained by Archimedes's method. The excitation spectra for the glass samples doped with Eu^{3+} were measured with a Hitachi F-4500 fluorescence spectrophotometer, monitoring the $^5D_0 \rightarrow {}^7F_2$ emission at 612 nm, the phonon sideband spectra can be observed at the high energy side of $^7F_0 \rightarrow {}^5D_2$ transition. The absorption spectra were obtained by using a VUV PC 3101 spectrophotometer (Shumandzu) at room temperature. The fluorescent decay curves of Er^{3+}: $^4I_{13/2} \rightarrow {}^4I_{15/2}$ were obtained by using the 980 nm pulsed output of an OPO laser (Continue, Sunlite) with 10 ns pulse duration, 10 Hz repetition frequency as excitation light, the fluorescent signals were passed to a spectrometer Triax 550 equipped with a semiconductor detector controlled by a personal computer. In the measurement of emission intensity the same experimental conditions were kept. In order to eliminate the re-absorption effect, the samples thinner then 1 mm were used, and the excitation light was focused on the sample margin in the measurement of emission spectra of $^4I_{13/2} \rightarrow {}^4I_{15/2}$ transition.

3. Results and discussion

3.1. Density and refractive index

Fig. 1a and b show the dependence of the density ρ, molar volume V_m and the refractive index n on the glass composition. The relative uncertainties for both the density and the molar volume are estimated to be less than 1%, and the error bars were represented in Fig. 1. It is found that with increasing the B_2O_3 content,

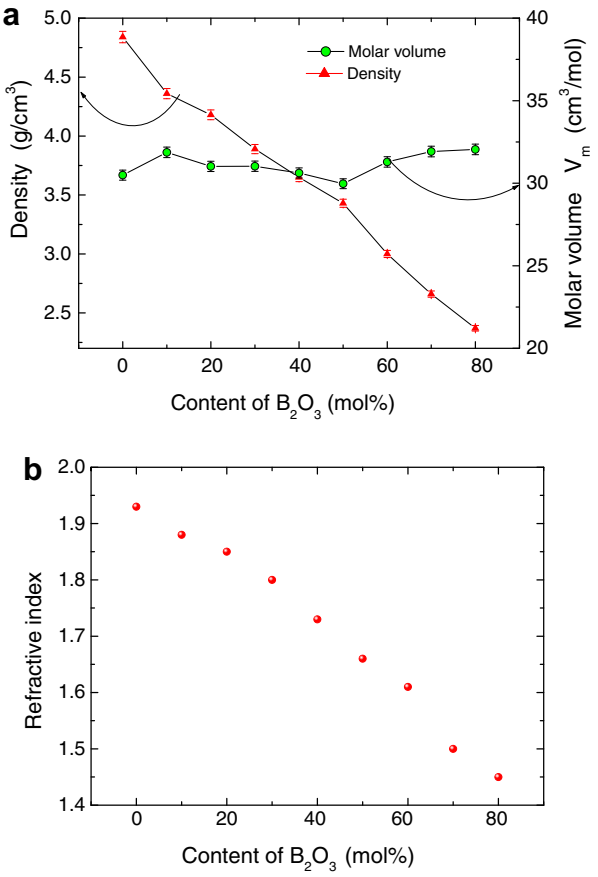

Fig. 1. Dependence of the weight density ρ, molar volume V_m (a) and the refractive indexes n (b) on the glass composition.

V_m increases first and then reaches its maximum at $x = 10$, after that decreases and reaches a minimum at $x = 50$, finally increases again. It is well known that the change of molar volume is associated with the change of the glass structure. According to Dell et al. model [23], one can confirm that for $x = 10$ all the Na^+ ions combine with BO_4 units surrounded by four TeO_4 units to form the structure of $NaBTe_4O_{10}$ like reedmergnerite in SBS glasses. So the molar volume shows a decrease because of the dense structure of $NaBTe_4O_{10}$, but the decrease of volume is not observed. A possible explanation for this behavior is the influence of Zn^{2+} ions on the different network structure of tellurite glasses. It is known that the introduction of modifier, ZnO, into the tellurite glass causes the structural transition $TeO_4 \rightarrow TeO_3$, and results in the formation of TeO_{3+1} polyhedron having one non-bridging oxygen atom [24–28]. Because of more non-bridging oxygen atoms in the glasses, only the nearly flat triangle BO_3 unit with one non-bridging oxygen atom is formed. In this case, the three-dimensional structure of tellurate glass is destroyed, thus, resulting in an increase of the molar volume. With further increasing the B_2O_3 content, BO_3 units are transformed into three-dimensional BO_4, which strengthens the structure, and the molar volume decreases [18]. When $x = 50$, BO_3 and BO_4 units in the glasses begin to mix together to form $BO_4(BO_3)_4$ groups, i.e., each BO_4 units is linked with four BO_3 units and BO_4 units reach the maximum. Thereby, the glass structure becomes the densest and displays the smallest molar volume. When $x > 50$, the additional B_2O_3 form extra BO_3 units which increase the molar volume.

It is known that the glass density is proportional to the average molecular weight of the glass and is inversely proportional to the molar volume. Fig. 1a shows that the fluctuation in the density va-

lue is opposite to the change in the molar volume, however, in a smaller range, the linear decrease in the average molecular weight with increasing B_2O_3 content plays an important role in modifying the density of the glasses.

Fig. 1b shows that the refractive index of the glass decreases monotonically as B_2O_3 content increases. It is well known that the refractive indexes are proportional to the electric polarizability and inversely proportional to the molar volume, as thus the high electric polarizability of Te–O bonds [24–28] has a stronger effect on the refractive index.

3.2. Phonon sideband spectra

In order to investigate the local structure of rare earth ions in these glasses the Eu^{3+} ions were doped into the glasses, since the phonon sideband (PSB) of Eu^{3+} ions is supersensitive to the evolution of the surroundings and can be clearly observed at the high energy side of $^7F_0 \rightarrow {}^5D_2$ transition [10]. Fig. 2 shows the dependence of phonon sideband (PSB) on the glass composition. The PSB spectra were fit to a linear combination of Gaussian's functions. Though the detailed interpretation of the phonon sideband (PSB) of borate–tellurite glasses is not easy due to their complexity originating from the different structural units, some reliable assignments of the PSB transitions were pointed out [7,28]. In Fig. 2a, the PSB spectra of Na_2O–ZnO–TeO_2 glass (pure tellurite) consist of four main bands: Two stronger bands at 680 and 770 cm^{-1} are due to the Te–O stretching vibrations of TeO_4 and TeO_3 structural units, and two weaker bands at 520 cm^{-1} and 930 cm^{-1} belong to the vibrations of Te–O–Te bridging bonds and $Te–O^-$ non-bridging bonds in TeO_3 structural units,

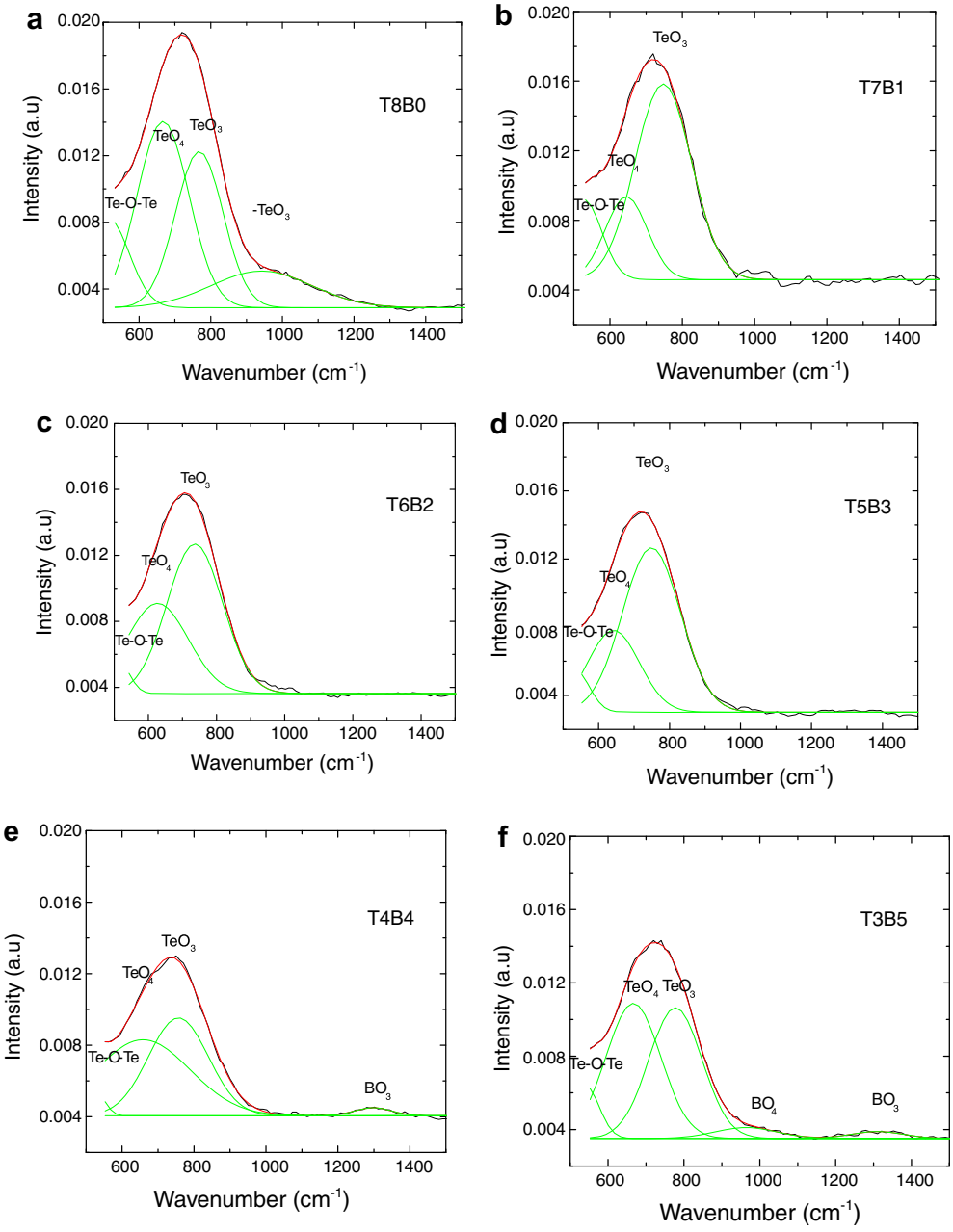

Fig. 2. The phonon sideband (PSB) spectra for the glasses with different compositions, Fig. 2 a–i are corresponding to the samples T8B0–T0B8. The sample number is marked in each figure.

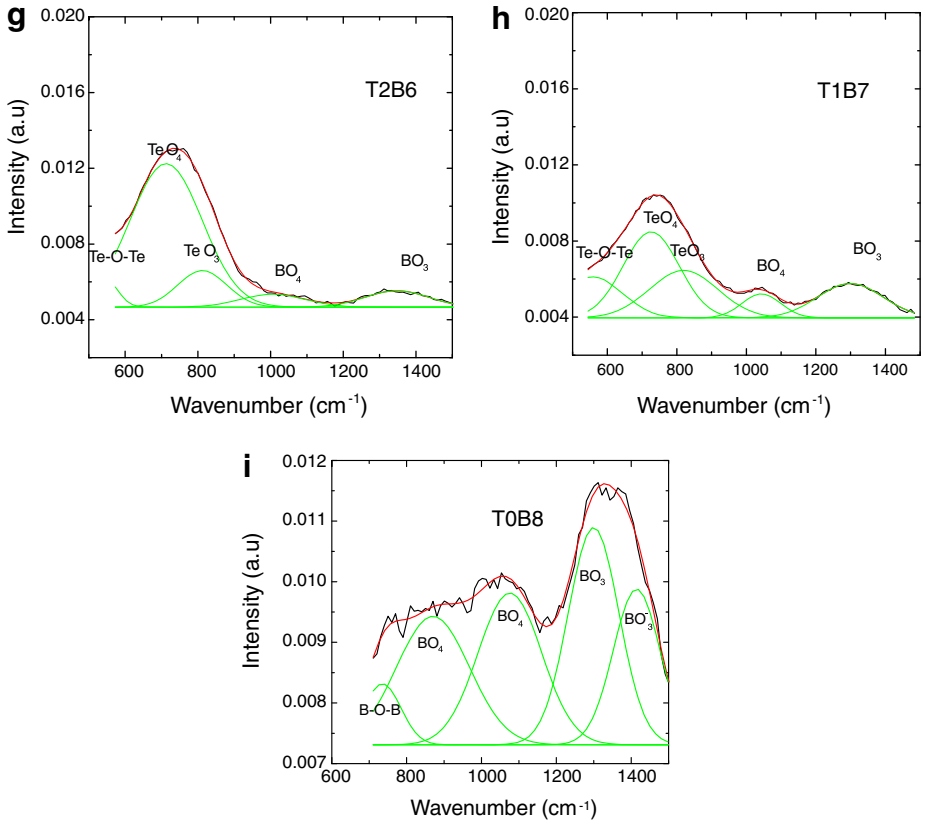

Fig. 2 (*continued*)

respectively. The PSB spectra of Na_2O–ZnO–B_2O_3 glass (pure borate) consist of five bands centered at about 1414, 1299, 1075, 870, 735 cm^{-1} (see Fig. 2i). The band centered at 1299 cm^{-1} and 1414 cm^{-1} can be attributed to the BO_3 units stretching vibrations, which are associated with the vibrational mode inside the various borate rings and the non-bridging B–O^-bonds, respectively. The lowest frequency band, 735 cm^{-1}, can be assigned to the bond bending vibration of the B–O–B linkage with the network, and the other two bands at 870, 1075 cm^{-1} are due to B–O stretching vibrations of tetragonal BO_4 units in the different structural groups. There is no new band appearing in the other glasses. The more detailed assignments of the various bands for other samples to the mode vibration are shown in Fig. 2b–h.

According to the research results by Y. Shimizugawa et al. [25], 930 cm^{-1} vibration band can be assigned to Te–O^- non-bridging bonds of TeO_3 units originating from modifying oxides ZnO. When x is larger than 10, the band responsible for the shift of non-bridging oxygen atoms disappears in the borate groups. The stronger vibration band of 770 cm^{-1} reflects that more TeO_3 units coupling with Eu^{3+} ions still exist in the glass host. As known that Eu^{3+} ions have a strong affinity towards the groups containing NBO, which is negative-charged, because they are readily available for charge compensation [19]. However, there are still a lot of Eu^{3+} ions existing in the tellurite groups when $x > 10$. They can be attributed to the influence of the lone-pair electrons (LPE) of tellurite groups [28]. Fig. 2 also shows that the ratio of the vibrational intensity of TeO_3 units and TeO_4 units change as the B_2O_3 content increases. This is because of the modifying influence of B_2O_3 on the structure of tellurite groups [24,25]. No vibration peaks of B–O bonds appear in the samples when $x = 10$–30, since less Eu^{3+} ions were bonded with boron and borate groups.

It is also found that the vibration intensity of Te–O bond decreases as the B_2O_3 content increases. This fact indicates that the Eu^{3+} ions enter the boron environment. The vibration band of BO_3 units appears until $x = 40$. This fact reflects that when B^{3+} ions are added, more Eu^{3+} ions enter the boron groups coupling with B–O bonds of BO_3 units. The vibration band of BO_4 units appearing at $x = 50$ is attributed to the increasing BO_4 units, which are transformed from BO_3 units as the B^{3+} ions increase. In Na_2O–ZnO–B_2O_3 glass, the band at about 1400 cm^{-1} can be assigned to the vibration of B–O^- non-bridging bonds of BO_3 units, thus indicating more non-bridging oxygen ions exist in the borate glass. Tanabe et al. [10] have pointed out that B–O-bonds are formed by an introduction of Eu^{3+} itself dominantly coordinate Eu^{3+} instead of a large number of boroxal rings.

3.3. Radiative, non-radiative relaxation rates and lifetimes

In our previous work [29], the optical transition calculations for all the samples doped with Er^{3+} ions were carried out based on the Judd–Ofelt (J–O) theory [30–34]. The dependency of optical transition intensity parameters on the glass composition was studied. This section is focused on the radiative, non-radiative relaxation and quantum efficiency of level $^4I_{13/2}$ of Er^{3+}.

According to J–O theory the radiative relaxation rate for $^4I_{13/2} \rightarrow {}^4I_{15/2}$ can be expressed as follows [35]:

$$A_{\mathrm{rad}} = \frac{16\pi^3 v^3 e^2}{3hc^3\varepsilon_0(2J+1)}\left[\frac{n(n^2+2)^2}{9}(0.019\Omega_2 + 0.118\Omega_4 + 1.462\Omega_6) + \frac{n^3}{4m^2c^2}|\langle f^N\psi J|L+2S|f^N\psi' J'\rangle|^2\right] \quad (1)$$

Because of the little contribution of Ω_2, Ω_4 to the value of A_{rad} Eq. (1) can be simplified as

$$A_{\mathrm{rad}} = \frac{16\pi^3 v^3 e^2}{3hc^3\varepsilon_0(2J+1)}\left[\frac{1.462n(n^2+2)^2}{9}\Omega_6 + \frac{n^3}{4m^2c^2}|\langle f^N\psi J|L+2S|f^N\psi' J'\rangle|^2\right] \quad (2)$$

where $\langle f^N\psi J|L+2S|f^N\psi' J'\rangle$ are the host-independent reduced matrix elements of the operator L + 2S. The first item on right hand in Eq. (2) increases proportionally to $n(n^2+2)^2\Omega_6$ and the second item increases proportionally to n^3. The fluorescent lifetime can be represented by [36]

$$\tau = \frac{1}{(A_{\mathrm{rad}} + W_{\mathrm{MP}} + W_{\mathrm{ET}})} \quad (3)$$

where A_{rad} is the radiative transition rate, W_{MP} and W_{ET} are the rates for multiphonon transition and energy transfer. Using Eq. (3) and the data of fluorescent lifetime and the radiative transition rate, $W_{\mathrm{MP}} + W_{\mathrm{ET}}$ can be derived. According to Toru Miyakawa's [37,38] theory the multiphonon transition rate can be expressed by

$$\begin{aligned} W_{\mathrm{MP}} &= W_0\exp(-\alpha\Delta E) & W_{\mathrm{ET}}(ab) &= W(ab)_0\exp(-\beta\Delta E)\\ \alpha &= (\hbar\omega)^{-1}\{\ln(p/g)-1\} & \beta &= (\hbar\omega)^{-1}\{\ln(p/g)-\ln(1+g_b/g_a)-1\}\\ & & p &\approx \Delta E/\hbar\omega \end{aligned} \quad (4)$$

where ΔE is the energy gap, W_0 and $W(ab)_0$ are the parameters corresponding to the decay rate at zero energy gap and zero phonon emission, a and b represent the interactional ions, g_a and g_b are the electron–phonon coupling constants of ions a and b, p is the number of phonons consumed in the non-radiative relaxation, and g is the electron–phonon coupling constant, which can be calculated by [10,38]

$$g = \frac{\int I_{\mathrm{PSB}}(\lambda)\mathrm{d}\lambda}{\int I_{\mathrm{PET}}(\lambda)\mathrm{d}\lambda} \quad (5)$$

where I_{PSB} is the intensity of the phonon sideband (PSB) spectra and I_{PET} is the intensity of pure electronic transition (PET). Fig. 3 shows the dependence of the radiative transition rate, non-radiative relaxation rate $W_{\mathrm{MP}} + W_{\mathrm{ET}}$, and $1/\tau$ on the B_2O_3 content. The insert is a plot of fluorescent lifetime (the experimental data can be found in Ref. [29]) versus the B_2O_3 content. It can be seen that with increasing B_2O_3 content: (1) the radiative transition rate decreases monotonously, but the difference between its maximum and minimum is not too large; (2) $W_{\mathrm{MP}} + W_{\mathrm{ET}}$, $1/\tau$ increase tardily when $x < 40$, and then increase rapidly when $x > 40$. The luminescence quantum efficiency can be obtained by using the normalized-thermal-lens method developed by Jacinto et al. [39,40]. The quantum efficiency can also be obtained from the following formula:

$$\eta = \tau A_{\mathrm{rad}} \quad (6)$$

where τ is lifetime and A_{rad} is the radiative transition rate. The quantum efficiencies of level $^4I_{13/2}$ for all the samples were calculated by using formula (6) and reported in our previous work [29]. The quantum efficiency decreases as the B_2O_3 content increases. In general, the introduction of B_2O_3 would improve the glass mechanical performance and its chemical stability. However, this is on the base of immolating partial quantum efficiency. It is also found that when introducing 10 mol% of B_2O_3, the quantum efficiency goes down to about 70%. Usually, 100% quantum efficiency is preferable, but the quantum efficiency is not the only factor under consideration. If this decrease in quantum efficiency is acceptable in the practical application, the introduction of B_2O_3 would be helpful for increasing glass host performance.

3.4. Up-conversation and down-conversion luminescence

Usually, up-conversion emission is in competition with the infrared down-conversion emission in Er^{3+} doped materials while upon 980 nm excitation. Effective elimination of the up-conversation luminescence may be benefit to the infrared down-conversion emission. The up-conversion fluorescent spectra for all the samples were measured upon 980 nm excitation and shown in Fig. 4. The most intense up-conversion emission is observed from the sample T8B0 (pure tellurite glass), and its intensity is about 40 and 100 times more intense than that of the sample T7B1 and T6B2, respectively. The up-conversion emission intensities for other samples are very weak. The dependence of integrated up-conversion emission intensity on the content of B_2O_3 was derived and plotted in a single log coordinate as the insert of Fig. 4. The intensity of up-conversation emission extremely decreases as the B_2O_3 content increases. It is also observed that the green emission is stronger than that of the red emission, thus indicating the energy transfer between Er^{3+} ions is weak [41] at the present doping level.

The down-conversion emission spectra for $^4I_{13/2}\rightarrow{}^4I_{15/2}$ transition were also measured for all the samples. The integrated emission intensities were calculated and the dependence of integrated emission intensity on the B_2O_3 content is shown in Fig. 5. It is observed that the integrated emission intensity of $^4I_{13/2}\rightarrow{}^4I_{15/2}$ transition decreases extremely with increasing the B_2O_3 content. The insert in Fig. 5 displays the normalized emission spectra for the samples with different contents of B_2O_3. The spectral

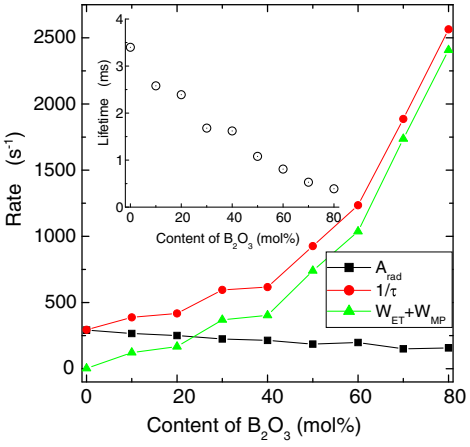

Fig. 3. Dependence of the radiative transition rate A_{rad} (for the transition $^4I_{13}\rightarrow{}^4I_{15/2}$), the summation W_{MP} + W_{ET} (W_{MP} is multiphonon relaxation rate, W_{ET} is energy transfer rate), and $1/\tau$ (τ is lifetime of level $^4I_{13/2}$) on the content of B_2O_3.

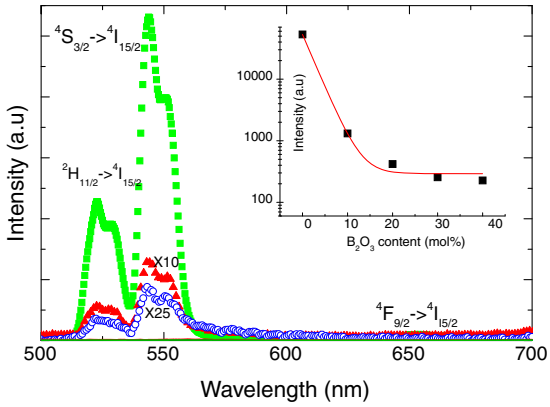

Fig. 4. The up-conversion emission spectra for the samples T8B0 (■), T7B1 (▲) and T6B2 (○); insert represents the relationship between integrated up-conversion emission intensity and the B_2O_3 content.

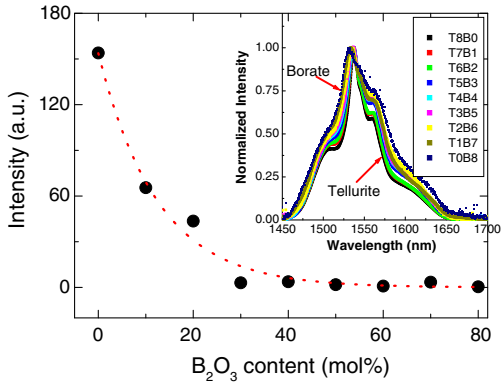

Fig. 5. The dependence of integrated down-conversion emission intensity on the B_2O_3 content, the insert shows the normalized emission spectra for the samples with various compositions.

bandwidth of $^4I_{13/2}\rightarrow{}^4I_{15/2}$ transition increases with increasing the B_2O_3 content. The effective spectral bandwidth Δ_{eff} can be estimated by using following formula:

$$\Delta_{eff} = \frac{\int I(\lambda)\mathrm{d}\lambda}{I_0(\lambda)} \tag{7}$$

where $I_0(\lambda)$ is the maximum intensity at the peak wavelength λ. The effective spectral bandwidths of sample T8B0 (pure tellurite glass) and T0B8 (pure borate) are estimated to be 61.1 and 89.6 nm, respectively. The effective spectral bandwidth of the other sample disperses between these two values, and increases with increasing the B_2O_3 content. Compared to the evolution trends of up-conversion and down-conversion emission intensities in Figs. 4 and 5, we can conclude that the up-conversation emission intensity attenuates more quickly than the intensity of $^4I_{13/2}\rightarrow{}^4I_{15/2}$ does. A similar phenomenon is also observed in Yb^{3+}/Er^{3+} co-doped silicate–borate glasses [42]. Therefore, introducing B_2O_3 into the tellurite glasses may be a better way to obtain a glass system with an increasing infrared spectral bandwidth, an emission efficiency of satisfying the practical application, and low up-conversion emission efficiency. It is worthwhile to mention that introducing B_2O_3 is probably not the direct reason causing an increase in the non-radiative transition rates between trivalent erbium levels. B_2O_3 introduction may increase OH^- content, which is an effective quencher for the Er^{3+} in the glasses, thus, the OH^- may be responsible for the increased non-radiative transition rates. This may be a further issue in our research work.

4. Conclusion

It was found that when a smaller content of B_2O_3 is introduced, B_2O_3 is transformed into BO_3 units because of large number of non-bridging oxygen ions from modifying oxides ZnO. No structure of $NaBTe_4O_{10}$ exists in the glass host. As the B_2O_3 content continues to increase the BO_4 units and BO_3 units begin to constitute $BO_4(BO_3)_4$ structures. When $x = 50$, BO_4 units reach maximum and all B^{3+} ions enter the structure of $BO_4(BO_3)_4$ to form the firmest structure. Rest B^{3+} ions will form BO_3 unit. We also investigated the dependence of radiative and non-radiative relaxation rate, lifetime and transition intensity of $^4I_{13/2}$ level as well as up-conversation emission on the glass composition. It is observed that the up-conversion emission intensity is more sensitive to the B_2O_3 content than that of 1.5 μm emission.

Acknowledgements

This work was partially supported by the NSFC (National Natural Science Foundation of China) (50572102, 50502131), Natural Science Foundation of Jilin Province (1999514, 20030514-2), Outstanding Young People Foundation of Jilin Province (20040113) and the Joint Program of NSFC-GACAC (General Administration of Civil Aviation of China) (60776814).

References

[1] D.D. Chen, Y.H. Liu, Q.Y. Zhang, Z.D. Deng, Z.H. Jiang, Mater. Chem. Phys. 90 (2005) 78.
[2] H. Lin, G. Meredith, S.B. Jiang, X. Peng, T. Luo, J. Appl. Phys. 93 (2003) 186.
[3] Y.G. Choi, D.S. Lim, K.H. Kim, Electron. Lett. 35 (1999) 1765.
[4] X. Feng, S. Tanabe, T. Hanada, J. Non-Cryst. Solids 48 (2001) 81.
[5] S. Hocdé, S.B. Jiang, X. Peng, N. Peyghambarian, T. Luo, Opt. Mater. 25 (2004) 49.
[6] X. Shen, Q.H. Nie, T.F. Xu, S.X. Dai, X.S. Wang, Spectrochim. Acta A 66 (2007) 389.
[7] A.H. Vcrhocf, H.W. den Hartog, J. Non-Cryst. Solids 182 (1995) 221.
[8] J. LorÖsch, M. Couzi, J. Pelous, R. Vacher, A. Levasseur, J. Non-Cryst. Solids 69 (1984) 1.
[9] C. Liu, C.A. Angell, J. Chem. Phys. 93 (1990) 378.
[10] S. Tanabe, S.T. Hirao, N. Saoga, J. Non-Cryst. Solids 122 (1990) 59.
[11] E.I. Kamitsos, G.D. Chryssikos, M.A. Karakassides, J. Phys. Chem. 91 (1987) 1067.
[12] E.I. Kamitsos, M.A. Karakassides, G.D. Chryssikos, J. Phys. Chem. 90 (1986) 528.
[13] E.I. Kamitsos, M.A. Karakassides, G.D. Chryssikos, J. Phys. Chem. 91 (1987) 107.
[14] L.M. Zhang, X.H. Huang, X.F. Song, Fundamentals of Materials Science, Press of Wuhan University of Technology, Wuhan, China, 2004.
[15] Z.Y. Zhang, N. Soga, Phys. Chem. Glasses 32 (1991) 43.
[16] J. Lorosch, M. Couzi, J. Pelous, R. Vacher, J. Non-Cryst. Solids 69 (1984).
[17] S. Tanabe, S. Todoroki, K. Hirao, N. Soga, J. Non-Cryst. Solids 122 (1990) 9.
[18] H. Doweidar, M.S. Meikhail, Phys. Chem. Glasses 31 (1990) 39.
[19] K. Gatterer, G. Pucker, H.P. Fritzer, Phys. Chem. Glasses 38 (1997) 293.
[20] Y.H. Yun, P.J. Bray, J. Non-Cryst. Solids 27 (1978) 63.
[21] Y.H. Yun, S.A. Feller, P.J. Bray, J. Non-Cryst. Solids 33 (1979) 73.
[22] S.Z. Xiao, J. Non-Cryst. Solids 45 (1981) 9.
[23] W.J. Dell, P.J. Bray, S.Z. Xiao, J. Non-Cryst. Solids 58 (1983).
[24] M.D. Pankova, Y. Dimitriev, M. Arnaudov, V. Dimitrov, Phys. Chem. Glasses 30 (1989) 260.
[25] Y. Shimizugawa, T. Maeseto, S. Inoue, A. Nukui, Phys. Chem. Glasses 38 (1997) 201.
[26] M. Arnaudov, Y. Dimitriev, Phys. Chem. Glasses 42 (2001) 99.
[27] D. Iliwva, V. Dimitriev, G. Bogachev, V. Krastev, Phys. Chem. Glasses 39 (1990) 241.
[28] A. Jha, S. Shen, M. Naftaly, Phys. Rev. B 62 (2000) 6215.
[29] Y. Yang, B. Chen, C. Wang, G. Ren, X. Wang, J. Rare Earths 25 (2007) 31.
[30] B.R. Judd, Phys. Rev. 127 (1962) 750.
[31] G.S. Ofelt, J. Chem. Phys. 37 (1962) 11.
[32] S. Tanabe, J. Non-Cryst. Solids 259 (1999) 1.
[33] S. Tanabe, J. Appl. Phys. 73 (1993) 8451.
[34] L. Pauling, J. Am. Chem. Soc. 51 (1929) 1010.
[35] D.K. Sardar, W.M. Bradley, J.J. Perez, J.B. Gruber, J. Appl. Phys. 93 (2003) 2602.
[36] Z.D. Pan, S.H. Morgan, K. Dyer, A. Ueda, J. Appl. Phys. 79 (1996) 8906.
[37] T. Miyakawa, K.L. Dexter, Phys. Rev. B 1 (1970) 2961.
[38] K. Soga, H. Inous, A. Makishima, J. Lumin. 55 (1993) 7.
[39] C. Jacinto, S.L. Oliveira, L.A.O. Nunes, J.D. Myers, M.J. Myers, T. Catunda, Phys. Rev. B 73 (2006) 125107.
[40] C. Jacinto, D.N. Messias, A.A. Andrade, S.M. Lima, M.L. Baesso, T. Catunda, J. Non-Cryst. Solids 352 (2006) 3582.
[41] N. Jaba, A. Kanoun, H. Mejri, A. Selmi, S. Alaya, H. Maaref, J. Phys.: Condens. Matter 12 (2000) 4523.
[42] G.E. Malashkevich, N.N. Ermolenko, V.I. Aleksandrov, M.A. Borik, G.M. Volokhov, A.S. Gigevich, G.A. Denisenko, A.V. Mazovko, V.N. Tadeush, Inorg. Mater. 23 (1987) 43.